

Structural Relaxation Taking Place in the Process of High-Field Magnetization

B. JEŹ^a, M. NABIAŁEK^{b,*} AND K. JEŹ^b

^a*Department of Technology and Automation, Faculty of Mechanical Engineering and Computer Science, Czestochowa University of Technology, al. Armii Krajowej 19c, 42-200 Czestochowa, Poland*

^b*Department of Physics, Faculty of Production Engineering and Materials Technology, Czestochowa University of Technology, al. Armii Krajowej 19, 42-200 Czestochowa, Poland*

Doi: [10.12693/APhysPolA.142.14](https://doi.org/10.12693/APhysPolA.142.14)

*e-mail: marcin.nabialek@pcz.pl

Structural relaxation plays a very important role in describing the magnetic properties of amorphous materials exhibiting soft magnetic properties. Changes in the position of the magnetization vector near short-range stresses can be investigated in amorphous materials using an indirect method called the ferromagnetic saturation approach. The analysis of the primary magnetization curves makes it possible to determine the type of stresses occurring in the volume of the tested alloys, which are in the form of free volumes and quasidislocation dipoles. The paper presents research on high-field primary magnetization curves for the FeCoB alloy.

topics: primary magnetisation curve, soft magnetic materials, magnetisation in strong magnetic fields

1. Introduction

Defects in crystalline materials are widely known and very well described in many scientific papers and academic textbooks [1, 2]. The impact of such defects on the properties of the tested alloys is very significant, and it can be concluded that they are a decisive factor in the formation of the resulting material parameters. Therefore, numerous methods of introducing or reducing defects in such materials are used. When it comes to amorphous alloys, it is difficult to find direct images showing defects in this structure. It has been shown previously that the obtained amorphous structure exhibits different properties for the same chemical composition, depending on the cooling rate between the liquid and solid states [3–7]. It should be added that amorphous materials are characterised by chemical and topological disorders — in contrast to crystalline materials [8–10]. These two factors affect direct changes in the properties of amorphous alloys. It is obvious that chemical and topological changes comprise a factor in the creation of areas described as heterogeneity of structure. These heterogeneities are sources of stress called defects. In amorphous materials, it is possible to study structural defects by an indirect method called the approach to ferromagnetic saturation. This method was adopted by H. Kronmüller [11–13]. The defects considered by H. Kronmüller are free volumes and quasidislocation dipoles. Free volumes play a similar role in

amorphous materials to point defects in amorphous materials. In contrast, quasidislocation dipoles are the equivalent of linear defects.

The aim of this study was to investigate the structure and impact of defects on the magnetisation process in strong magnetic fields, in the area called the approach to ferromagnetic saturation. Samples of the amorphous alloy $\text{Fe}_{43+x}\text{Co}_{29-x}\text{Y}_8\text{B}$ (where $x = 0$ or 5) were produced and tested, each sample being in the form of a plate with a thickness of 0.5 mm.

2. Materials and methods

The samples for testing were made from high purity component elements: Fe — 99.99%, Co — 99.99%, Y — 99.95%, B — 99.9%. Boron was added in the form of a FeB alloy. The weighed alloy components were melted in an arc furnace under an argon atmosphere. The molten components were remelted four times on each side, which promoted good homogenisation of the alloy. Then, the resulting ingots were divided into smaller pieces, which were used to provide melt samples for research. Using a method involving a suction of liquid alloy into a water-cooled copper mould (suction casting), samples were obtained in the form of plates, each with a thickness of 0.5 mm and an area of 100 mm². After fragmentation using a low-energy process, these plate samples were subjected to structural analysis. The structure was studied using a BRUKER D8

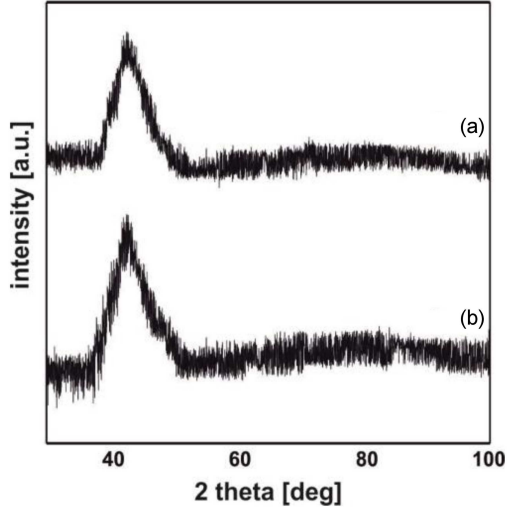


Fig. 1. X-ray diffractograms obtained for the alloy samples: (a) $\text{Fe}_{43}\text{Co}_{29}\text{Y}_8\text{B}_{20}$, (b) $\text{Fe}_{48}\text{Co}_{24}\text{Y}_8\text{B}_{20}$.

Advance X-ray diffractometer, which was equipped with a cobalt lamp ($\text{Cu } K_{\alpha_1} \lambda = 1.54433$). The samples were measured in the range of 2θ angle from 30 to 100° with a measuring step of 0.02° and an exposure time of 5 s. The tests of resulting magnetic properties were carried out using a Lakeshore 7307 VSM vibration magnetometer. Primary magnetisation curves and static magnetic hysteresis loops were measured. Based on analysis of the static magnetic hysteresis loops, values of saturation magnetisation and coercivity field were determined. Analysis of the primary magnetisation curves, measured at the appropriate density, was performed according to the assumptions of H. Kronmüller's theorem. All tests were performed at room temperature for samples in the post-solidification state.

3. Results

Figure 1 shows the X-ray diffraction images measured for the tested alloys. The obtained diffractograms are typical for materials with an amorphous structure. Only wide maxima in the 2θ range of 40 – 50° are visible. Figure 2 shows static magnetic hysteresis loops for the studied alloys.

Based on the hysteresis loops, the values of the coercivity field H_C and saturation magnetisation M_S were determined (see Table I). Based on the shapes of the static magnetic hysteresis loops, it can be stated that the $\text{Fe}_{48}\text{Co}_{24}\text{Y}_8\text{B}_{20}$ alloy is easier to magnetise than the $\text{Fe}_{43}\text{Co}_{29}\text{Y}_8\text{B}_{20}$ alloy, which is indicated by a higher value of magnetisation at the same value of the intensity of the external magnetic field. Figure 3 shows the magnetization curves, as a function $(\mu_0 H)^{-1}$, for the alloys under study.

In both cases, the process of magnetisation in high values of intensity of the external magnetic field is associated with the rotation of the magnetisation vector in the vicinity of linear defects. For

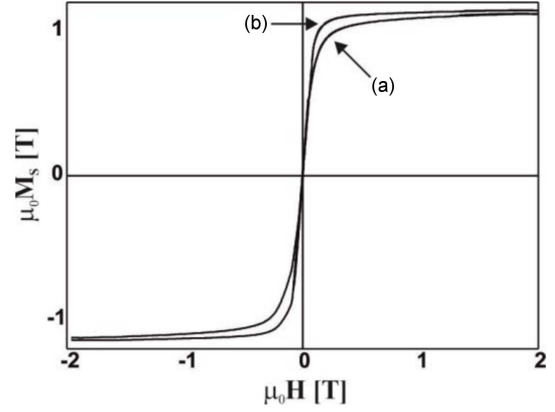


Fig. 2. Static magnetic hysteresis loops for the alloys: (a) $\text{Fe}_{43}\text{Co}_{29}\text{Y}_8\text{B}_{20}$, (b) $\text{Fe}_{48}\text{Co}_{24}\text{Y}_8\text{B}_{20}$.

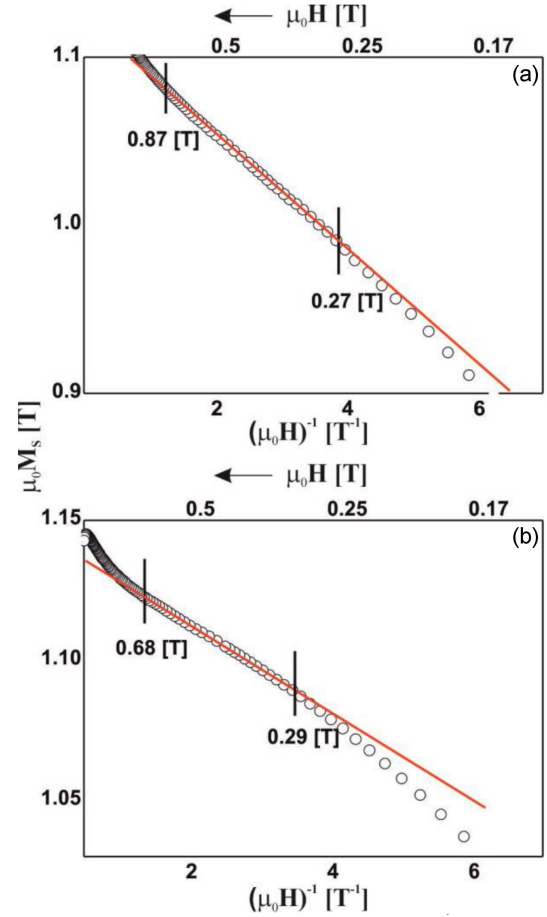


Fig. 3. Magnetisation, as a function of $(\mu_0 H)^{-1}$, for the alloy samples (in the form of 0.5 mm plates): (a) $\text{Fe}_{43}\text{Co}_{29}\text{Y}_8\text{B}_{20}$, (b) $\text{Fe}_{48}\text{Co}_{24}\text{Y}_8\text{B}_{20}$.

the $\text{Fe}_{43}\text{Co}_{29}\text{Y}_8\text{B}_{20}$ alloy, this phenomenon occurs in the range of magnetic field strength from 0.27 to 0.87 T, while for the $\text{Fe}_{48}\text{Co}_{24}\text{Y}_8\text{B}_{20}$ alloy, the equivalent range is from 0.29 to 0.68 T. A narrower range of effect of linear defects on magnetisation suggests a slightly different structure of the alloy.

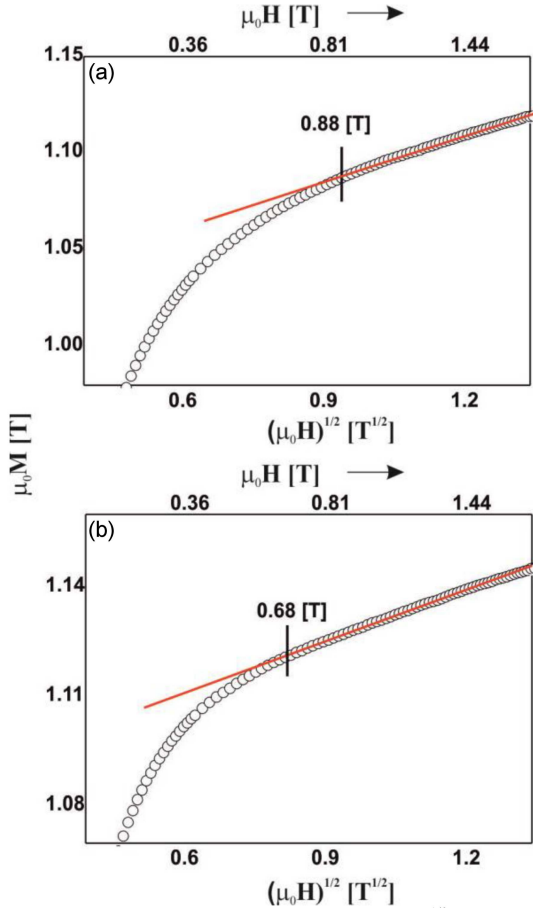


Fig. 4. Magnetisation as a function of $(\mu_0 H)^{1/2}$, for the alloy samples (in the form of 0.5 mm plates): (a) $\text{Fe}_{43}\text{Co}_{29}\text{Y}_8\text{B}_{20}$, (b) $\text{Fe}_{48}\text{Co}_{24}\text{Y}_8\text{B}_{20}$.

TABLE I

Magnetic properties of the $\text{Fe}_{43+x}\text{Co}_{29-x}\text{Y}_8\text{B}_{20}$ alloys.

Alloy	M_S [T]	H_C [$\frac{\text{A}}{\text{m}}$]	D_{spf} [meV nm ²]
$\text{Fe}_{43}\text{Co}_{29}\text{Y}_8\text{B}_{20}$	1.12	140	34
$\text{Fe}_{48}\text{Co}_{24}\text{Y}_8\text{B}_{20}$	1.14	75	50

Figure 4 shows the magnetisation curves as a function of $(\mu_0 H)^{1/2}$. The process of magnetisation of the above approach area to ferromagnetic saturation is associated with the suppression of thermally induced spin waves (the so-called Holstein–Primakoff paraprocess) [14]. Based on the shape of the curve, the spin-wave stiffness parameter D_{spf} was determined. The values are given in Table I.

The shapes of the X-ray diffractograms, the shapes of the static magnetic hysteresis loops, and the type of structural defects occurring, indicate great similarity of the tested alloys. However, the determined parameters indicate substantially superior magnetic properties of the $\text{Fe}_{48}\text{Co}_{24}\text{Y}_8\text{B}_{20}$ alloy — almost twice the lower value of the coercivity

field and a higher value of saturation magnetisation. The increase in the D_{spf} parameter is associated with the improvement of exchange interactions between pairs of magnetic atoms Fe–Fe, Co–Co and Fe–Co.

4. Conclusions

The aim of this study was to investigate the influence of Fe and Co content on the structural and magnetic properties of rapidly cooled alloys produced by the suction-casting method. The results show that the addition of Fe atoms, at the expense of Co atoms, facilitates an easier magnetisation process. A higher Fe content increases the homogeneity of the alloy, as indicated by a lower value of coercivity field and the concentration of the influence of linear defects on the magnetisation process over a narrower range of external magnetic field intensity.

References

- [1] M. Jaraiz, L. Pelaz, E. Rubio, J. Barbolla, G.H. Gilmer, D.J. Eaglesham, H.J. Gossmann, J.M. Poate, *MRS Online Proceedings Library (OPL)* **532**, 43 (1998).
- [2] C.R.A. Catlow, *Defects and Disorder in Crystalline and Amorphous Solids*, Springer-Science+Business Media, Madrid 1994.
- [3] S. Abdia, M. Samadi Khoshkhood, O. Shuleshova et al., *Intermetallics* **46**, 156 (2014).
- [4] P. Pietrusiewicz, M. Nabiałek, B. Jež, *Materials* **13**, 4962 (2020).
- [5] M.-N. Avettand-Fenoel, M. Marinova, R. Taillard, W. Jiang, *J. Alloys Compd.* **854**, 157068 (2021).
- [6] K. Gruszka, M. Nabiałek, M. Szota et al., *Arch. Metall. Mater.* **61**, 641 (2016).
- [7] S. Garus, M. Nabiałek, J. Garus, *Acta Phys. Pol. A* **126**, 960 (2014).
- [8] A. Zhu, G.J. Shifflet, S.J. Poon, *Acta Mater.* **56**, 593 (2008).
- [9] Z. Su, T. Shi, H. Shen, L. Jiang, L. Wu, M. Song, Z. Li, S. Wang, C. Lu, *Scr. Mater.* **212**, 114547 (2022).
- [10] K. Błoch, M. Nabiałek, M. Dośpiał, S. Garus, *Arch. Metall. Mater.* **60**, 7 (2015).
- [11] P. Sikora, M. Nabiałek, K. Błoch et al., *Acta Phys. Pol. A* **139**, 582 (2021).
- [12] H. Grimm, H. Kronmüller, *Phys. Status Solidi B* **117**, 663 (1983).
- [13] H. Kronmüller, *IEEE Trans. Magn.* **15**, 1218 (1979).
- [14] T. Holstein, H. Primakoff, *Phys. Rev.* **58**, 1098 (1940).